VI International Conference on Computational Methods in Marine Engineering
MARINE 2015
F. Salvatore, R. Broglia and R. Muscari (Eds)

DYNAMICAL SIMULATION AND OPTIMIZATION OF DOUBLE-HELICAL AUV

JANIS AUZINS*, MARCIS EIMANIS*

* Institute of Mechanics
Riga Technical University
6 Ezermalas Street, LV-1006, Riga, Latvia
e-mail: auzinsjp@latnet.lv, http://www.mi.rtu.lv

Key words: Autonomous underwater vehicles, Surrogate modeling, Helical drive.

Abstract. The paper presents an original design of autonomous underwater vehicles where thrust force is created by the helicoidal shape of hull rather than screw propellers. The contra-rotating bow and stern parts create propulsion force. The middle part of the vehicle, which is built from elastic material, contains a Cardan joint which controls bending drives (actuators). The controlled bending of the hull allows the maneuvering of the vehicle. A bending drive velocity control algorithm for the automatic control of the vehicle movement direction is proposed. The dynamics of AUV are simulated using multibody simulation software MSC Adams. For the simulation of water resistance forces and torques the surrogate polynomial metamodels are created on the basis of computer experiments with CFD software. The simulation results are compared with measurements of the AUV prototype, created at Institute of Mechanics of Riga Technical University. Experiments with the prototype showed good agreement with simulation results and confirmed the effectiveness and the future potential of the proposed principle.

1 INTRODUCTION

In traditional underwater vehicles, the propulsive force is usually obtained by using propellers. In past years in many autonomous underwater vehicles (AUV) the principle of fish-movement body/caudal fin propulsion – the flexion wave - has been implemented. But in the world of bacteria, a different principle is followed – rotation of all parts of the body. Bacteria *Spirillum volutans, Spirochaetes* and many others move by rotating flexible parts of the body – one or many *flagellas* [1]. At present there exist several scientific works on the simulation of flexible flagella motor-actuated bacteria dynamics and some physical experiments have been done with rotation of flexible helical tail constructions [2]. Currently there is no known functioning AUV that works on the basis of this principle. Contra-rotating propellers (CRP) are well established as one of the most efficient technologies [3], but here we study contra-rotating parts of hull. The fact that all vehicle parts are in rotation is not acceptable for vehicles transporting human beings. However, for AUV's equipped with a rapid control system this is not a significant obstacle. At Riga Technical University the design of AUV was developed using two reflection-symmetric parts with a helical shape. The parts are connected with motorized rotational joints. The vehicle contains a central part (see Fig.1) with the hull built from elastic material. The central part contains a Cardan (universal) joint with two servomotors. The motorized Cardan joint implements the two-directional bending of

the hull and allows maneuvering the vehicle. The direction control algorithm uses angular orientation sensor information. The simulation of the underwater dynamics of a rapidly rotating and bending vehicle is a hard problem. The rotation causes turbulence and vortex motion of the fluid and a very complex interaction between the fluid and the vehicle body and between parts of the vehicle. Currently it is possible to simulate only a straight motion of the vehicle with commercial CFD software and the simulation is very time-consuming. The ICP/TP connection between multibody software and CFD software [4] is possible, but the stability and accuracy of such a calculation approach is highly dubitable. Therefore the dynamics of the AUV with 10 degrees of freedom was simulated using the multibody system simulation software MSC Adams. The fluid-mechanism interaction was simulated using metamodels of water resistance forces and moments, obtained by approximation of results of numerical experiments with CFD software Flow-3D.

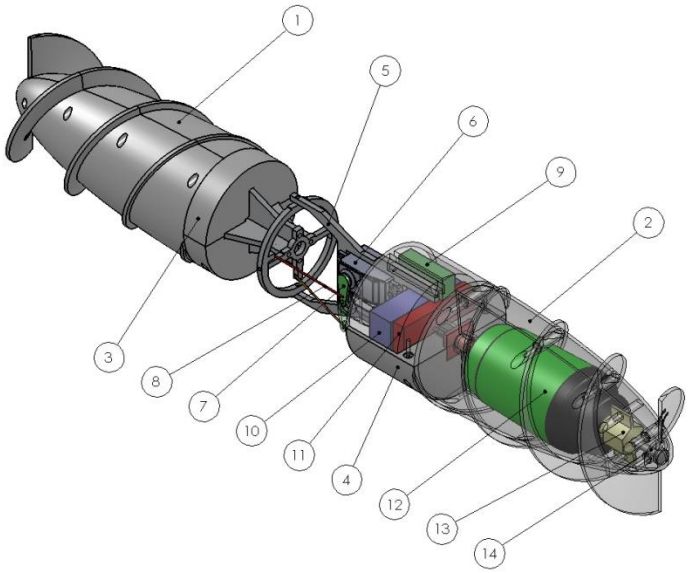

Figure 1: The structure of Durbis-2. 1, 2 – rear and front screw, 3 – mid-body front part, 4 – mid-body rear part, 5 – cross/ vector kite gimbal, 6 – servo, 7 – servo connector, 8 – shaft connecting connector and gimbal ring, 9 – analog signal receiver, 10 – battery, 11 – PDM type speed controller for DC motors, 12 – hull with DC motor and reducer, 13 – drive shaft, 14 – screw axis.

2 THE CONTROL OF HELICOIDAL AUV WITH BENDING JOINTS

The control principle of the AUV Durbis-2 is based on bending the Cardan joint in such a way that the rotation axis of the bow (front) screw would be oriented in the target direction. The rotation axis for tilting the bow screw from current position to the required direction is perpendicular to screw rotation axis unit vector b and to vector a from the center of vehicle to the target. The unit vector T of this finite rotation is equal to the cross product of both vectors, divided by the norm of vector $\boldsymbol{a}$. (see. Fig. 2)

$$\boldsymbol{T} = \frac{1}{\|\boldsymbol{a}\|}\boldsymbol{b} \times \boldsymbol{a} \tag{1}$$

However, it should be taken into account that the control drive torques q_z and q_y are intrinsic,

and the rear part of the vehicle will bend in opposite direction. We assume that the control system is equipped with sensors that give both current angles φ_y and φ_z of the servo-drives, as well as the projections of direction vector $\boldsymbol{a}$ on the axis of the central coordinate system (fixed on the Cardan journal cross). The control servo drives can implement the required angle or rotation speed. In the case of speed control, the relatively simple control law can be realized:

$$\begin{cases} \dot{\varphi}_y = -k_c arcsin(T_y) \\ \dot{\varphi}_z = k_c arcsin(T_z) \end{cases} \tag{2}$$

where k_c – constant coefficient. The control algorithm can use the vehicle linear velocity vector instead of axis vector $\boldsymbol{b}$. The main practical problem is the sensor system, which should include three-axis orientation sensors, because the middle part (middle body) can rotate around the longitudinal axis of vehicle. This fact makes simple manual control of the vehicle with two direction controllers impossible, because due to rotation the turn φ_z for the middle body is not always equal to yaw and φ_y is not always equal to pitch rotation.

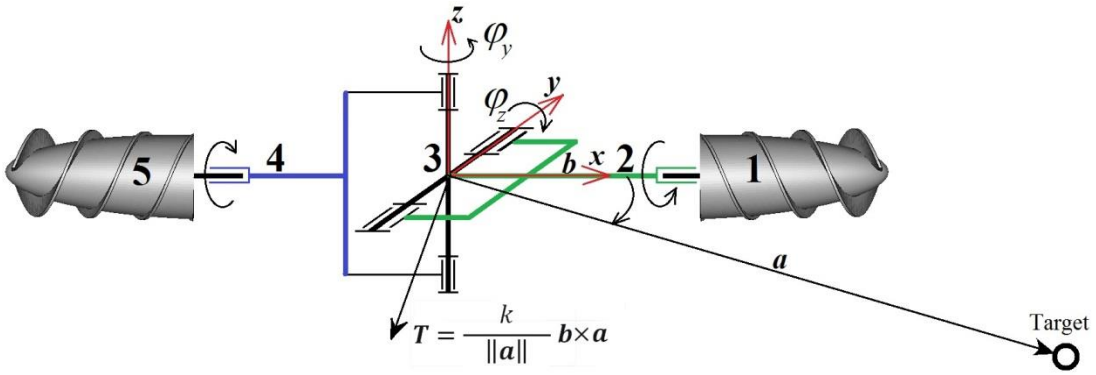

Figure 2: Kinematic diagram of Durbis-2. 1, 5 – bow and stern screws, 2 and 4 front and rear drive sections, 3 – Cardan journal cross (spider), φ_y, φ_z – tilt angles around Cardan joint axes, $\boldsymbol{a}$ – vector from the middle point of the Cardan joint to the target point, $\boldsymbol{a}$ – unit vector of bow screw rotation axis.

3 CREATION OF SURROGATE MODELS OF WATER RESISTANCE

Since it is practically impossible to simulate a moving mechanism with 10 degrees of freedom in CFD programs taking into account full interaction between fluid and mechanism links, in practice the metamodeling (surrogate modeling) technology is broadly applied [5]. This implies the creation of simplified models of water resistance, obtained by planned experiments with CFD software. There are several good review papers that describe different aspects of surrogate modeling and advantages to numerous methods and they provided the background to choose the appropriate method [6, 7]. The authors of [5] used the classic Response surface method based on second order polynomial approximations of computer experiments with CFD software ANSYS FLUENT.

We used the software EDAOpt for design, analysis and optimization of computer experiments, created at Riga Technical University [8]. The polynomial surrogate models for water resistance forces $\boldsymbol{F}_i$ and torques $\boldsymbol{T}_i$ are created in the form

$$\boldsymbol{F}_i = -A_i^{\mathrm{T}} \boldsymbol{V}_i - \|\boldsymbol{V}_i\| B_i^{\mathrm{T}} \boldsymbol{V}_i \tag{3a}$$

$$\boldsymbol{T}_i = -C_i^{\mathrm{T}}\boldsymbol{\omega}_i - \|\boldsymbol{\omega}_i\| D_i^{\mathrm{T}}\boldsymbol{\omega}_i \tag{3b}$$

where $\boldsymbol{F}_i$ – column-vector of total water resistance force on the i-th body, $\boldsymbol{T}_i$ – column-vector of total water resistance torque acting about the center of mass of the i-th body, $\boldsymbol{V}_i$ - column-vector of translation velocity of center of mass of i-th body, $\boldsymbol{\omega}_i$ - column-vector of translation velocity of center of mass of i-th body, A_i, B_i, C_i, D_i – columns of coefficients, obtained by least-square approximation. All vector projections are calculated in body (moving) coordinate systems. When creating such surrogate models, the flow change from vehicle bending in the Cardan joint is not taken into account.

4 SIMULATION OF RECTILINEAR MOTION

Commercial CFD software ANSYS FLUENT, COMSOL Multiphysics, STAR-CD, Flow-3D and others provide limited capacity for modelling fluid-mechanism interaction dynamics. In these programs it is possible to insert into a fluid flow rigid bodies with all 6 degrees of freedom or constrain the motion excluding some translation or rotation degrees. So-called General Moving Object (GMO) components can be of a mixed motion type, namely have translational and/or rotational velocities that are coupled in some coordinate directions and prescribed in the other directions. A body-fixed reference system ("body system"), defined for each moving object, and the space reference system ("space system") are employed. Therefore these rigid bodies can be coupled with the ground using rotational or translational joints. Unfortunately, it is not possible to connect two moving bodies among themselves using rotational joints.

To model rectilinear motion using software Flow-3D we used the following approach. Three main parts: bow (front) screw, middle body and stern (rear) screw are placed in alignment, allowing only rotation around longitudinal axis x. The middle body is standing still. In this model none of the three parts have any contact with each other and there are no contact forces or friction forces between them.

An external torque Q around x-axis acts on the bow screw and the opposite torque $-Q$ acts on the stern (right) screw. The mesh domain size in y and z directions was built in accordance with the recommendations given in [9] - approximately 1.4 times larger than the diameter of vehicle. We used the specified pressure conditions instead of wall-type boundary conditions. We used the idea that is applied in all wind tunnel experiments – the object may be moving through a stationary fluid, or the fluid may be flowing past a stationary object—these two are effectively identical since, in principle, it is only the frame of reference of the viewer which differs. In our simulations the vehicle is placed in such a way that its center of mass is fixed in the inertial coordinate system and the water flows past a stationary vehicle. CFD software calculates the fluid pressure and velocity in all mesh points as well as the total resistance forces and torques acting on all GMOs. The program also calculates the reaction forces and torques created by motion constraints. In our case there are three components of support reaction force and two components of reaction torque for each part of vehicle. The most important are the reaction force components in longitudinal direction, the other forces and torques are relatively negligible. In order to assume that the modelled movement is equivalent to vehicle swimming with constant drive torques $q_1 = q_2 = Q$, it is necessary that the sum of reaction forces (called *residual control x-force* in the program Flow-3D [10, 11]) in

longitudinal direction would be equal to zero (see Fig. ?):

$$R_{x1} + R_{x2} + R_{x3} = 0 \tag{4}$$

This condition can be satisfied only by experimentally determining the (external) drive torque value Q for each given fluid velocity value V_x , trying out different software input settings.

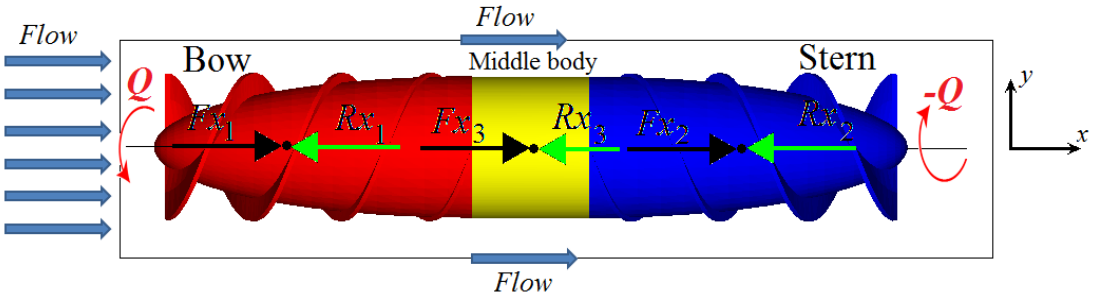

Figure 3: Top view of Durbis-2 in the finite volume mesh of the software Flow-3D

The Chen-Kim modification of Renormalized group (RNG) k-ε model [10, 12] has been used for turbulence modeling with following coefficient values:

$$(\sigma_k, \sigma_\varepsilon, C_{\varepsilon 1}, C_{\varepsilon 2}, C_\mu, \beta) = (0.7194, 0.7194, 1.42, 1.68, 0.0845, 4.38, 0.012) \tag{5}$$

Figures 4, 5 shows the water streamlines and flow horizontal velocity contours for the fluid common velocity 0.6 m/s. It can be seen, that the rear screw works inefficient and pulls along the water behind it.

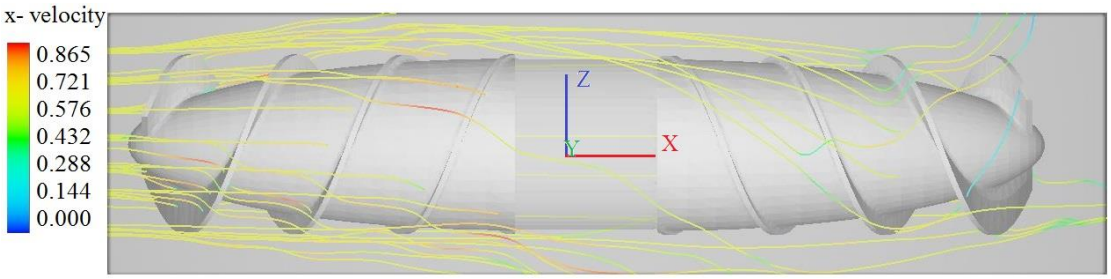

Figure 4: Water streamlines around Durbis-2. Velocity 0.6 m/s

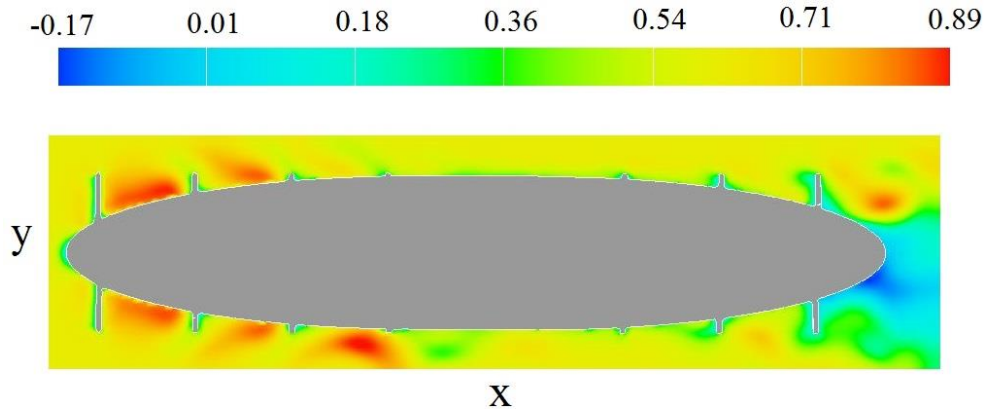

Figure 5: Fluid x-velocity contours in the middle section

Figure 6 shows the stabilization of rotational velocity of bow and stern screws and the oscillation of summary longitudinal reaction force for the given flow velocity 0.6 m/s and drive torque 0.146 Nm.

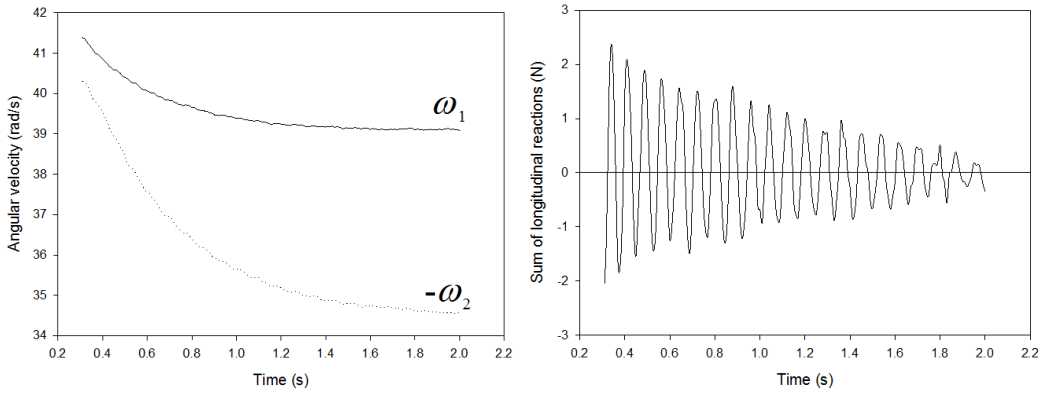

Figure 6: Stabilization of the screw rotation speed (left) and summary support reaction (right)

Figure 7 shows the approximated dependence of the drive torque on the velocity of rectilinear motion. Only four numerical experiments were used for obtaining this second order polynomial approximation. The adjusted R-square criterion value is 0.9997 and the value of the *relative leave-one-out-crossvalidation* [8] is 5.3%, confirming the high adequacy of the approximation. The second order polynomial approximation contains a linear term that is insignificant in practice, see Pareto chart [8, 13 p. 264] Fig. 8.

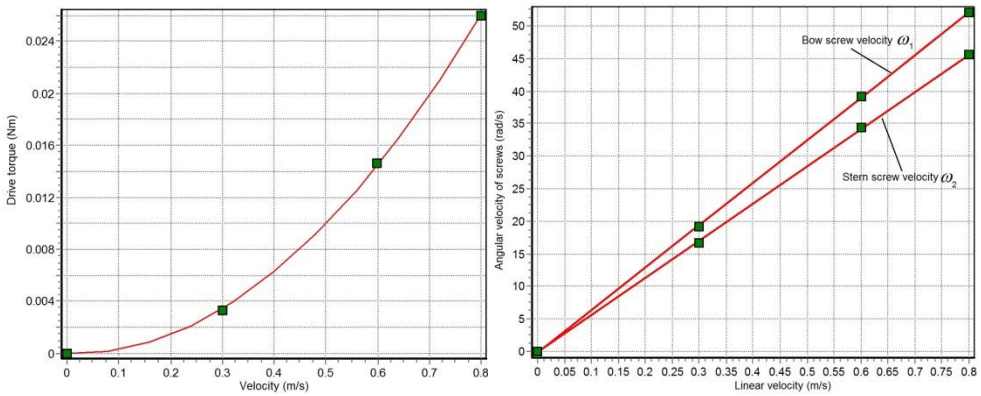

Figure 7: Approximate dependence of drive torque (left) and screw angular velocity (right) on the linear velocity of AUV

The right graph of Fig. 7 shows the approximated linear dependence between the velocity of rectilinear motion and angular velocities of bow and stern screws. The relative cross-validation error of approximation is about 1%. As can be seen, at equal (opposite) drive torques, the rear screw rotates significantly slower than the bow (front) screw. The fluid pressure and shear force analysis showed that the contribution of the rear screw in the creation of the thrust force is also significantly smaller.

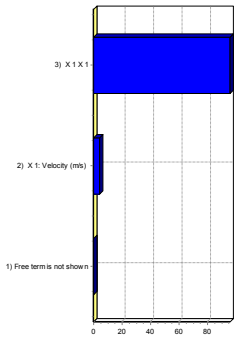

Figure 8: Pareto plot for the torque dependence approximation

The transverse motion velocity during turns of vehicle is much smaller than the longitudinal speed. The surrogate water resistance force models were created by simulation of flow acting in the perpendicular direction. The water resistance torques around the transversal axis were calculated under the assumption that they are created by distributed pressure, proportional to squared velocity.

If the resistance force in the transverse direction can be approximated as $F_y = -k_y V_y^2$, then the simplest approximation for resistance torque for rotation around the perpendicular axis through middle point of prolonged object will give $T_z = -\frac{k_y L^3}{32}\omega_z^2$, where T_z – the resistance torque around z-axis, ω_z – the angular speed of rotation around z-axis, L – the length of body in longitudinal direction. Of course, this is a highly simplified approximation that does not take into account the interaction of rotation and translation movement, added mass effects, flow changes from them connected adjacent body parts.

5 FULL DYNAMIC SIMULATION WITH MSC ADAMS

MSC Adams is world's most famous and widely used 3D Multibody Dynamics (MBD) software tool for dynamical analysis of mechanisms and machines, including mechanisms with rigid and flexible links, drive and control system. The mathematical model in the form of internal systems of differential-algebraic equations is built automatically according to the kinematic diagram which can be imported from any CAD software. Here we used MD Adams 2011, ID C00FD03A-BB49AF41.

The simulated mechanism contains 5 rigid-body links, connected with 4 rotational joints, see Fig. 9, 10.

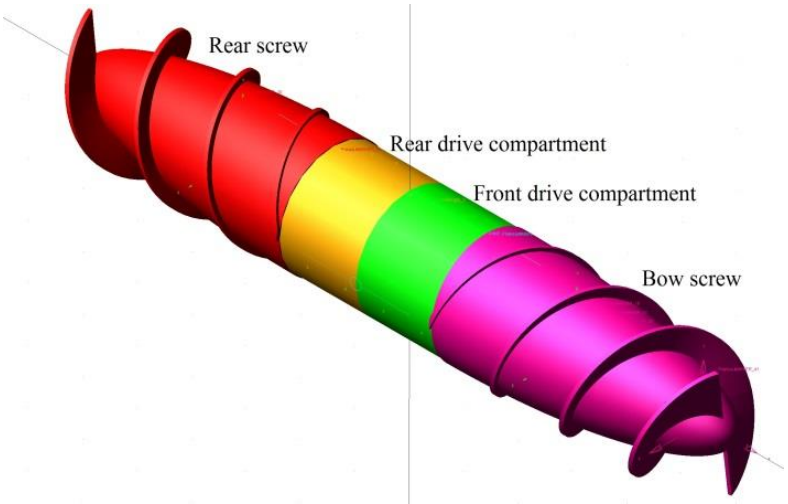

Figure 9: Durbis-2 in MSC Adams. Outside view. Cardan journal cross not shown

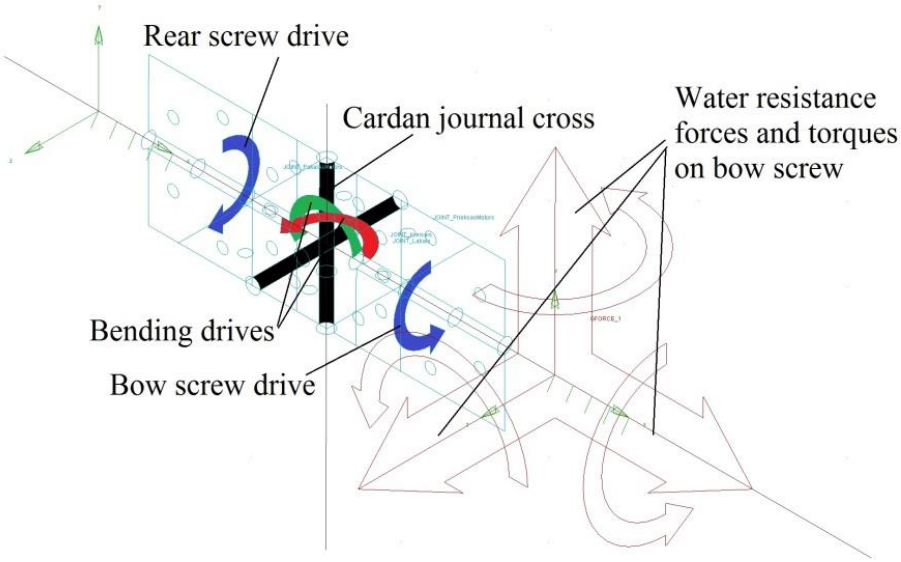

Figure 10: Durbis-2 in MSC Adams. The inner structure

Therefore the model has 10 degrees of freedom. The water resistance forces and torques are given as external forces, using the created surrogate models and the possibilities of the function builder in MSC Adams. Fig. 11 shows the "General force" property for the bow

screw, which is in fact the realization of quadratic approximation of flow simulation results (3a, 3b).

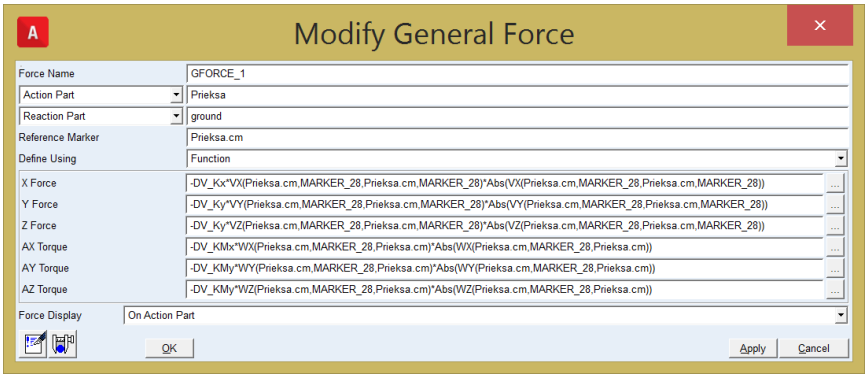

Figure 11: Water resistance surrogate model

The thrust and bending electro-drive dynamics were not simulated in detail. It was assumed that the thrust drives generate the necessary torque and orientation drives generate the necessary rotation speed. The angular velocity of bow and rear screws was varied in the range from zero to 20 RPM. When modelling rectilinear motion, at ±10 RPM the linear velocity of vehicle was obtained as about 0.6 m/s. Figure 12 shows the vehicle following a target, using an automatic control law (2). The spherical target moves in three dimensions according to sinusoidal law $x(t) = 0.7\sin(0.5t)$, $y(t) = 0.7\cos(0.5t)$, $z(t) = 0.46\sin(1.5t)$. The optimal value of the coefficient of control law (2) k_c =110 was found using computer experiments.

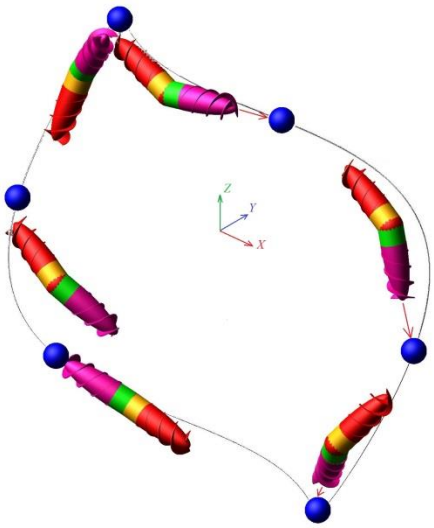

Figure 12: Following a moving target

6 PROTOTYPE OF DURBIS-2 AND VALIDATION

The physical prototype of the AUV DURBIS-2 was built in the master thesis of Marcis Eimanis [14] using CAD software SolidWorks and the Mass Portal 3D Printer Pharaoh Delta. The bow and stern screws were printed using PLA plastic. The screws are rotated with an

LN22 Series electro drive individually connected to each screw (2 drives in total), using 7.4V Lipo battery, the reducer generates ~600 RPM and torque of about 0.06 Nm (controlled by *pulse-duration modulation*).
Direction is controlled by 2 servo motors: Blue Bird High speed BSM-706, low profile (torque at 4.8V – 0.46 Nm; speed at 4.8V – 8 rad/s at no load). Low profile servo motors were deliberately chosen to obtain additional free space for other components.

The middle bending body consists of a Cardan-type cross construction, the material is 4mm thick EN-AW-5754 aluminum with an elastic silicone cover.

Figure 13: The prototype Durbis-2

The middle body is water-proof and may be used as a "cargo compartment". The drive body is located on the central shaft that turns the spindle connected with the screw, causing it to rotate. The central shaft is fixed in a stationary position at the ends of the middle body.

Model dimensions: total length 590mm, maximum diameter together with the screw 87.25mm, maximum diameter of hull 84mm, length of screw 190 mm, pitch of helix 106 mm.

The range for the Cardan bending angles is ±30°. The prototype is not equipped with orientation sensors; therefore it is controlled using a 40 MHz, 4.5-7.5V receiver placed in the vehicle body and a three-component control transmitter console. Due to the absence of middle body vertical orientation control and a sensor system for the prototype, an additional mass was placed in the lower part of the middle body to avoid its rotation around the longitudinal axis. This allows good remote control of the prototype. The remote control is possible at a distance of about 20 meters and at about 2 m depth of submergence.

The prototype Durbis-2 demonstrated very good maneuverability. The only measured parameters were linear velocity (about 0.6 m/s) and angular velocity of screws (about 600-700 RPM). This gives good agreement with simulation results from CFD and multibody dynamic simulation software. The real velocity and maneuverability of Durbis-2 is so high that the vehicle can move vertically and almost jump out of the water like a fish (see Fig. 14).

Figure 14: Durbis-2 „jumping" out of water

7 CONCLUSIONS

- The numerical and physical simulation results have proved the functionality, maneuverability and energy efficiency of the proposed propulsion principle and control system. It must be noted that this principle can be used not only for underwater vehicles, but also for devices that move in granular, loose ground, as well in pipes filled with fluid, including blood vessels. The experiment's measurements are compared with the results predicted using the computational model. The comparison shows that the model can predict with reasonably good accuracy the dynamic performance of the AUV with double helicoid hull shape.
- Further research should include more accurate analysis of the turbulence and cavitation effects, and study the possibility to build an internal angular orientation sensor system based on MEMS technology.
- Shape optimization of the hull and both screws would also be necessary. With the current design where the vehicle has almost completely symmetrical bow and stern parts, the stern screw has a mostly supportive function and the main thrust force is created by the bow screw. If the symmetry principle is abandoned, it would be possible to create a more energy-efficient shape for the double-helical vehicle.

8 ACKNOWLEDGEMENT

This work has been supported by the European Social Fund within the Project No. 2013/0025/1DP/1.1.1.2.0/13/APIA/VIAA/019 "New "Smart" Nanocomposite Materials for Roads, Bridges, Buildings and Transport Vehicles".

REFERENCES

[1] Eisenbach, M. Bacterial Chemotaxis. In: eLS. John Wiley & Sons Ltd, Chichester, (2011).
[2] Flores, H., Lobaton, Méndez-Diez, E.S., Tlupova, S., Cortez, R. A study of bacterial flagellar bundling, *Bulletin of Mathematical Biology*, **67**, 137-168, (2005).
[3] Caponnetto, M., 2000. Optimisation and Design of Contra-Rotating Propellers. In SNAME Propellers/Shafting Symposium. Virginia Beach, Virginia, pp. 3-1 to 3-9, (2000).
[4] Elliott, A., Slattengren, J., and Buijk, A., Fully Coupled Fluid/Mechanical Response Prediction for Truck-Mounted Tank Sloshing Using Cosimulation of MSC.ADAMS® and MSC.Dytran®, SAE Technical Paper 2006-01-0932, 2006, doi:10.4271/2006-01-0932.
[5] Carroll, J and Marcum, D. Developing a Surrogate-Based Time-Averaged Momentum

Source Model from 3D CFD Simulations of Small Scale Propellers. Lecture Notes in Engineering and Computer Science: Proceedings of The World Congress on Engineering, London, United Kingdom, July 2013, pp. 1622–1627, (2013).

[6] Forrester, A. and A. J. Keane, A. . Recent advances in surrogate-based optimization. *Progress in Aerospace Sciences*, vol. **45**, January 2009, pp. 50–79.

[7] Queipo, N. V., Haftka, R.T., Shyy, W., Goel, T., Vaidyanathan, R. and Tucker, P.K. Surrogate-based analysis and optimization. *Progress in Aerospace Sciences*, vol. **41**, 2005, pp. 1–28.

[8] Auzins, J., Janushevskis, A., Janushevskis, J., Skukis, E. Software EDAOPT for Experimental Design, Analysis and Multiobjective Robust Optimization. OPT-i International Conference on Engineering and Applied Sciences Optimization, Geece, Kos, 4.-6. June, 2014. Athens: National Technical University, 2014, pp. 101-123, (2014).

[9] Watanabe T., Kawamura T., Takekoshi Y., Maeda M., Rhee S. H. Simulation of steady and unsteady cavitation on a marine propeller using a RANS CFD code. Fifth International Symposium on Cavitation (CAV2003), Osaka, Japan, 1-4 November 2003, pp. 1-4, (2003).

[10] Flow Science, Inc., FLOW-3D user's manual, 10.1 edition, Flow Science, Inc., Santa Fe, N.M., (2011).

[11] Wei, G. A fixed-mesh method for general moving objects in fluid flow. *Modern Physics Letters B*, Vol. **19**, Issue 28-29, pp. 1719-1722 (2005).

[12] Chen, Y.S. and Kim, S.W. Computation of Turbulent Flow Using an Extended K-E Turbulence Closure Model. NASA Report, CR 179204, October (1987).

[13] Montgomery, D., C. *Design and Analysis of experiments*. 8th Edition, John Wiley & Sons, (2013).

[14] Eimanis, M. Development of new type propulsion device for underwater vehicles, Master thesis, Riga Technical University, (2014), https://ndr.rtu.lv/lv/view/11681/